Composites: Part A 185 (2024) 108311

Contents lists available at ScienceDirect

Composites Part A

journal homepage: www.elsevier.com/locate/compositesa

A novel approach to design structural natural fiber composites from sustainable CO_2-derived polyhydroxyurethane thermosets with outstanding properties and circular features

Guillem Seychal [a,b], Pierre Nickmilder [c], Vincent Lemaur [d], Connie Ocando [a], Bruno Grignard [e,f], Philippe Leclère [c], Christophe Detrembleur [e], Roberto Lazzaroni [d], Haritz Sardon [b], Nora Aranburu [b,*], Jean-Marie Raquez [a,*]

[a] Laboratory of Polymeric and Composite Materials, Center of Innovation and Research in Materials and Polymers (CIRMAP), University of Mons, Place du Parc 23, Mons, 7000, Belgium
[b] POLYMAT and Department of Advanced Polymers and Materials: Physics, Chemistry, and Technology, Faculty of Chemistry, University of the Basque Country UPV/EHU, Paseo Manuel de Lardizabal 3, Donostia-San Sebastián, 20018, Spain
[c] Laboratory for Physics of Nanomaterials and Energy (LPNE), Research Institute for Materials Science and Engineering, University of Mons (UMONS), 20 Place du Parc, B-7000 Mons, Belgium
[d] Laboratory for Chemistry of Novel Materials, Research Institute for Materials Science and Engineering, University of Mons, Place du Parc 23, Mons, 7000, Belgium
[e] Center for Education and Research on Macromolecules (CERM), CESAM Research Unit, University of Liege, Sart-Tilman B6a, 4000 Liege, Belgium
[f] FRITCO$_2$T Platform, University of Liege, Sart-Tilman B6a, 4000 Liege, Belgium

ARTICLE INFO

Keywords:
A: Natural fibers
A: Polymer-matrix composites (PMCs)
B: Interface/interphase
CO_2-based thermosets

ABSTRACT

We herein propose capitalizing on strong hydrogen bonding from novel bio-CO_2-derived dynamic thermosets to achieve high-performance natural fiber composites (NFC) with circular features. CO_2- and biomass-derived polyhydroxyurethane (PHU) thermosets were selected, for the first time of our knowledge, as matrices for their ability to make strong H-bond, resulting in outstanding mechanical properties for NFC. Exploiting this H-bond key feature, exceptional interface bonding between flax and PHU was confirmed by atomic force microscopy and rationalized by atomistic simulation. Without any treatment, an increase of 30% of stiffness and strength was unveiled compared to an epoxy benchmark, reaching 35 GPa and 440 MPa respectively. Related to the thermoreversible nature of hydroxyurethane moieties, cured flax-PHU were successfully self-welded and displayed promising properties, together with recyclability features. This opens advanced opportunities that cannot be reached with epoxy-based composites. Implementing CO_2-derived thermosets in NFC could lead to more circular materials, critical for achieving sustainability goals.

1. Introduction

Natural cellulosic fibers (NF) such as flax, hemp, or sisal are deemed to replace glass fibers in many composite applications [1]. Their attractiveness lies in their renewability, high specific mechanical properties [2], low environmental footprint [3], and cost-effectiveness [2], particularly in the context of structural materials. Despite the significant advances in natural fiber composites (NFC) over the last decades, finding eco-friendly polymer matrices, particularly fully bio-based thermoplastics and thermosets, remains challenging. For instance, fully bio-sourced thermoplastics, such as polylactic acid (PLA), present limited interfacial affinity with NF, leading to poor mechanical properties for the resulting composites [4]. Although the surface treatments of fibers are beneficial for the adhesion quality, these are hampered by high costs, sustainability concerns, and scalability issues, and may provoke undesirable decreases of other composite properties [4]. By contrast with their thermoplastic counterparts, bio-sourced thermosets afford better adhesion strength [5], resulting in composites with higher mechanical performances. Among them, the combination of epoxy-amine (EP) resins with NFs has delivered structural composites whose remarkable performances [6] result from the presence of H-bonds and the potential reaction between oxirane and hydroxyl moieties [5]. However, the sustainability of structural composites, particularly their poor environmental footprint, remains a severe concern. While a few bio-based thermosets have made their way into the market or are

* Corresponding authors.
E-mail addresses: nora.aramburu@ehu.eus (N. Aranburu), jean-marie.raquez@umons.ac.be (J.-M. Raquez).

https://doi.org/10.1016/j.compositesa.2024.108311
Received 25 March 2024; Received in revised form 18 May 2024; Accepted 9 June 2024
Available online 13 June 2024

being explored for structural applications [7], the demand for greener, safer, and more high-performing alternatives persists. One notable example of progress in this direction is the utilization of a partially bio-based epoxide, i.e. GreenPoxy from Sicomin [8,9], which is a bisphenol A-type resin obtained from bio-based epichlorohydrin. While solutions to green the fabrication of structural composites are quickly progressing [10], addressing the end-of-life scenario of such epoxy composites is challenging, yet being mainly related to energy recovery and landfilling [11].

In this context, the utilization of poly(hydroxyurethanes) (PHU), a non-isocyanate polyurethane family [12], has gained growing attention in materials science. Easily accessible from precursors of bio- and CO_2-origin, these resins display on-demand modular and high-performance properties. Being considered viable alternatives to conventional polyurethanes (PUR) made from carcinogenic, reprotoxic, and mutagenic isocyanates as their main PUR precursor [13], PHUs are obtained from the step-growth reaction of polyamines with polycyclic carbonates (CC). Cyclic carbonates are produced through an efficient, and cost-effective transformation of (bio-)epoxides precursors with CO_2 under solvent- and purification-free conditions [14]. Structurally, PHUs differ from PURs by the presence of hydroxyl moieties pendant along the main chain skeleton, providing hydrophilicity to the resins [13] while favoring the ability of PHU chains to create multiple hydrogen bonds, which is of particular interest for NFCs.

Besides the high potential for their biobased production, the hydroxy-urethanes formation is reversible and these linkages can be involved in transcarbamoylation reactions, a rearrangement mechanism that makes PHUs adaptive networks [15]. Such covalent adaptative networks (CAN) can be potentially recycled, upcycled, or reprocessed under appropriate conditions [15–17]. Recent discoveries have illustrated the utility of PHUs as an alternative to isocyanate-based polyurethanes, despite being limited yet to academia. Additionally, PHUs have thus far been merely considered as replacements for isocyanate-based polyurethanes in their conventional applications [18], i.e., as adhesives, coatings, or (self-blowing) foams, while their promising properties could be major assets in other applications.

To the author's best knowledge, PHUs have never been investigated in the realm of sustainable composites, particularly for NFC, nor compared to their epoxide counterparts. Capitalizing on the intrinsic PHU features, a new generation of recyclable composite materials from biocarbon and/or CO_2 origin with remarkable thermo-mechanical performances could be designed. The hydrophilic nature of PHU and the presence of additional OH moieties should create resins with better affinity for NF while proposing a viable end-of-life recyclability scenario through repurposing of the structural composites through hot compression molding.

The wide structural diversity of PHU precursors [19] has already allowed the construction of PHU thermosets with adaptable thermo-mechanical properties [20], mostly for adhesives [21], coatings [22] and foams [23]. However, no thermosetting PHU formulations are responding to the requirements of the composite industry in terms of processability and material performance. Interesting carbonate precursors, such as pentaerythritol- [20] or trimethylolpropane-based [20,24] CCs have delivered PHUs with promising properties for composite applications. In such applications, the expected performances include a strain at break exceeding 3%, slightly larger than those of structural natural fibers [2] and Young's modulus ranging from 1 to 4 GPa. In a recent study [24], our research team highlighted the complex crosslinking behavior through a rheological study of these bio-based CCs cured with m-Xylylene diamine. Although reactive PHU formulations may face high viscosity and long curing times issues in the realm of composite manufacturing, at the current development stage, they remain promising platforms with many advantages. Especially, their high thermo-mechanical properties and reprocessability, remain of particular interest for NFCs. In our previous work, PHU thermosets with high modulus and stress were developed while maintaining satisfactory ductility. Glass transition temperatures over 60 °C were obtained, comparable to most of the current market solutions [25]. Notably, all formulations proved to be reprocessable under catalyst-free conditions through a simple thermo-mechanical procedure. These interesting features open new doors in terms of manufacturing and end-of-life of such bio-based composites.

In this work, we propose the use of this unique PHU chemistry to manufacture unidirectional flax-based laminates by thermocompression. Trimethylol Propane Carbonate (TMPTC) was chosen as a sustainable precursor due to its appropriate properties for NFCs and sufficient flowing characteristics suitable for composite manufacturing. Trimethylol propane can be derived from starch and sugars through enzymatic processes [20]. Subsequent bio-epoxy can be obtained from the epoxidation of (bio)polyols with glycerol-derived epichlorohydrin. m-Xylylene diamine (MXDA), a potentially furfural-derived diamine [26], was considered as the curing agent. It is important to note that due to the low availability of biobased amines, the one used in this work remains oil-based. The neat PHU thermoset was characterized and compared to an epoxy counterpart made from trimethylolpropane triglycidyl ether. Notably, CCs being obtained from epoxide monomers, such precursors can be also polymerized by aminolysis enabling the direct comparison between the material properties made from both epoxy or CC precursors. The reaction schemes are presented in Fig. 1. Unidirectional flax laminates were then manufactured and deeply characterized from morphology to mechanical performance. The study was completed by Atomic Force Microscopy and quick atomistic simulations to better understand the interactions at the interface of the PHU and flax. Their fire behavior was also assessed as a major requirement in structural applications. Finally, taking advantage of the dynamicity of the hydroxyurethanes in PHU networks, single-ply flax-PHU sheets were cured and later welded as pre-preg materials.

2. Materials and methods

2.1. Sample preparation

2.1.1. Materials

Trimethylol Propane Triglycidyl Ether (TMPTE, DENACOL EX321, biobased grade, Epoxy Equivalent Weight EEW = 140 g/eq) was kindly supplied by DENACOL NAGASE Chemtex. 1,8-Diazabicyclo[5.4.0] undec-7-ene (DBU), Tetrabutylammonium iodide (TBAI), and 4-(dimethylamino) pyridine (DMAP) were purchased from Sigma-Aldrich. m-Xylylene Diamine (MXDA) was bought from TCI. Air Liquide provided the carbon dioxide. All chemicals were used as received without any further purification. Flax fiber tape (FlaxTape UD110, 110 $g.m^{-2}$) was purchased from EcoTechnilin. Carbon fiber quasi-unidirectional tape (CF-UD100, Pyrofil TR50S 15k, 100 $g.m^{-2}$) was purchased from Mitsubishi. Trimethylolpropane triglycidyl carbonate (TMPTC) was synthesized at the kilogram scale following an already-reported procedure [24], details are reported in supporting information.

2.1.2. Synthesis of the epoxy and polyhydroxyurethane thermosets

To expedite the curing process of PHU, 1 mol% of DMAP was used as a catalyst. The choice of catalyst and load was made based on an internal study, which revealed no alterations in the network structure or final properties but enhanced the curing process. Related results from this study can be found in the second section of the supporting information.

All epoxy and PHU thermosets were cured with an equimolar ratio of reactive functions in a similar procedure as reported elsewhere [24]. The precursors were degassed under vacuum at 60 °C for one hour before use. The PTFE molds were preheated at 60 °C. After adding the MXDA hardener to the monomer, the mixture was mixed manually for 5 min. The homogeneous mixture was poured into the mold of the wanted shape and pressed at 80 °C and 3 bar for 2 h followed by one hour at 100 °C in an oven. A final post-curing of 1 h at 150 °C was performed to complete the curing.

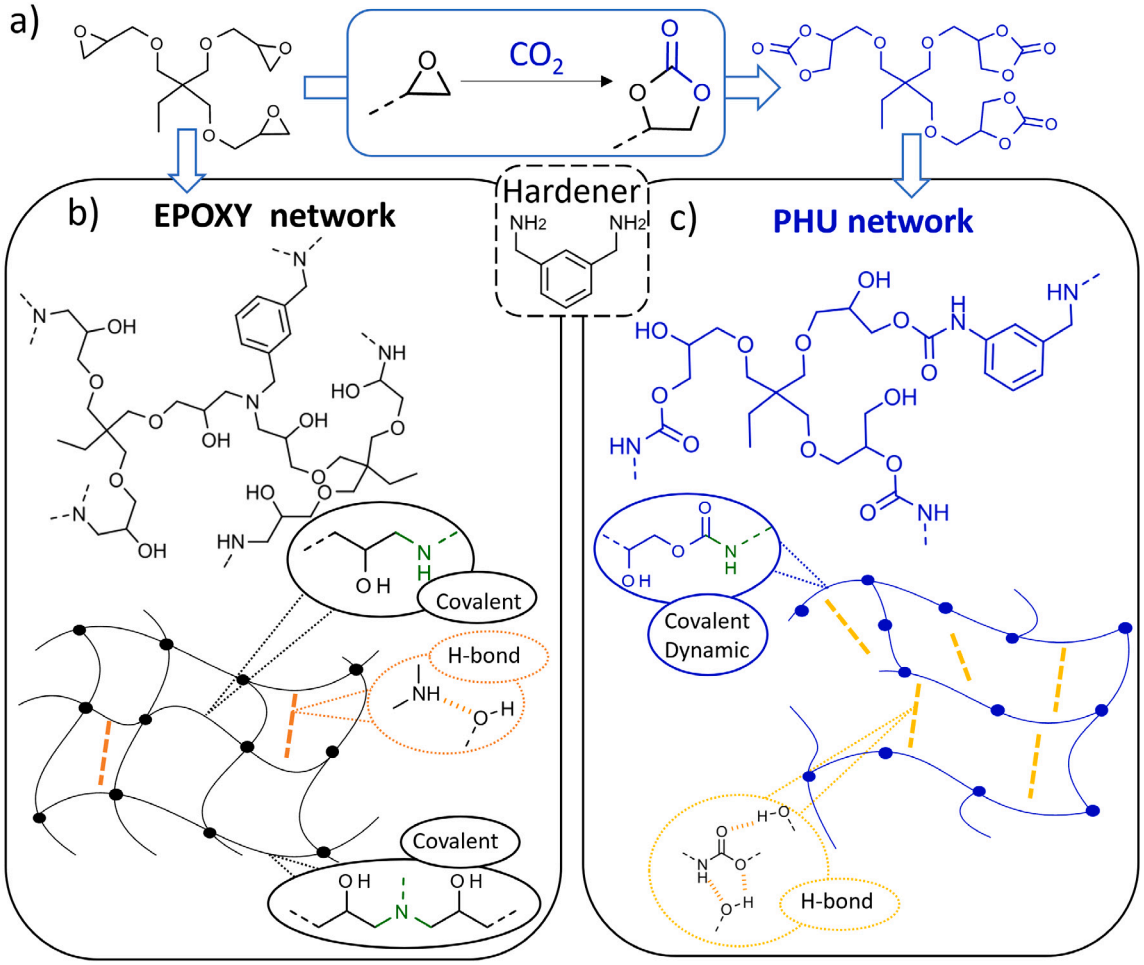

Fig. 1. (a) Formation of cyclic carbonate by addition of CO_2 to epoxy, (b) Epoxy-amine representative network, and (c) PHU representative network. (Full line insets represent the network crosslinking node, and dotted line insets represent the potential inter-/intra-molecular H-bond formed.).

2.1.3. Unidirectional composite manufacturing

Flax unidirectional hand lay-up laminates (200 × 150 mm^2) were manufactured by thermocompression with a $[0]_6$ stacking sequence. To impregnate the fibers, the epoxy-amine and CC-amine mixture were prepared by weighting about 1.4 times the mass of fibers. The plies were stacked in a 60 °C preheated Teflon-coated steel mold with a line of resin. This process was reported to provide high fiber volume content with fairly viscous resins and natural fibers [27]. The two axial edges were left free to allow air and matrix excess to flow out. The mold was gradually pressed to 4 bar to ensure an entire impregnation of the fibers and cured following the protocol described in Section 2.1.2, i.e. 2 h at 80 °C, followed by 1 h at 100 °C. The post-curing was conducted in an oven after unmolding for 1 h at 150 °C. The flax-PHU and flax-epoxy composite are referred to as F-PHU and F-EP, respectively.

Sections were precisely cut from the obtained plates using a metallic guillotine to prepare the samples. Before testing, these samples were conditioned at 23 °C and 50% RH to guarantee moisture equilibrium. The fiber mass was estimated from the reinforcement areal weight using Eq. (1). Fiber volume fraction (V_f) was calculated using Eq. (2) and void content (V_v) was calculated using Eq. (3).

$$m_f = n \times A_r \times S \tag{1}$$

$$V_f = \frac{\frac{m_f}{\rho_f}}{\frac{m_f}{\rho_f} + \frac{m_c - m_f}{\rho_m}} \tag{2}$$

$$V_v = 1 - \rho_c\left(\frac{w_m}{\rho_m} + \frac{w_f}{\rho_f}\right) \tag{3}$$

in which n is the number of plies, S is the sample's surface, and A_r is the reinforcement areal weight. ρ_x, m_x, and w_x refer to the density, the mass, and the weight fraction respectively. f subscript refers to fibers, m to the matrix, and c to the composite. Flax' density was fixed at 1.39 g.cm^{-3}. Matrix density values were measured in ethanol using Archimedes's principle.

2.1.4. Welding of flax-PHU pre-preg

Single-ply laminates were manufactured under the same condition described in Section 2.1.3. The single-ply thick sheet was then cut into 70 × 70 mm^2 square. Six plies were then stacked into an adapted steel mold with a Teflon protective layer. After a preheating step of 15 min in a press at 160 °C, 3 kT force (around 6 MPa) was applied. Both temperature and pressure were maintained for 15 h to efficiently weld the laminates. The obtained plate was then unmolded and cut into three-point bending test samples with a guillotine. The protocol was fixed to ensure the best results given the previously obtained conditions published in [24].

2.2. Characterization

Detailed information on the experimental characterization can be found in section I.3 of the supporting information.

2.3. Analytical and numerical models

2.3.1. Theoretical modulus calculations

To normalize the experimental values and thus obtain an estimation of the adhesion efficiency, the Chamis' micromechanical model [28]

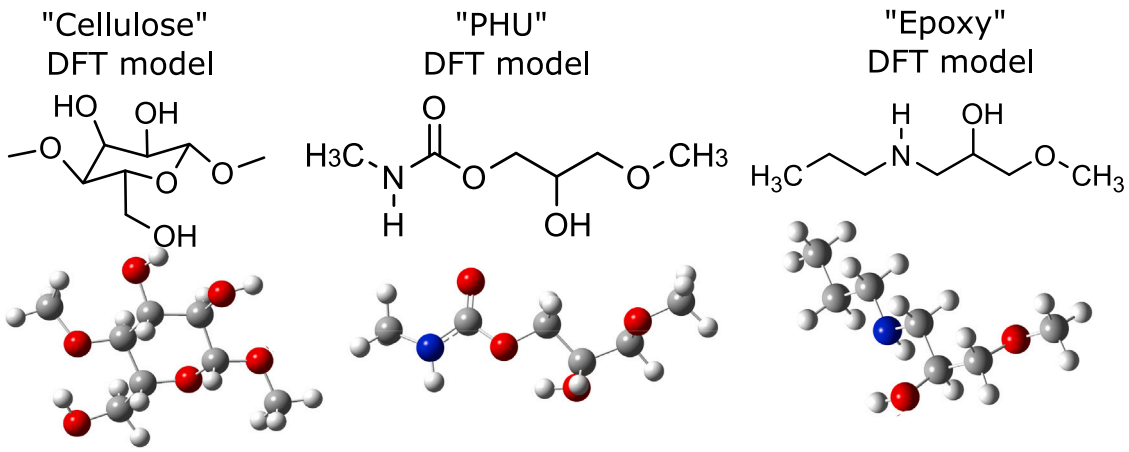

Fig. 2. Representation of the used structures for the atomistic simulations.

was used. Chamis' model was preferred to the traditional Rule-Of-Mixture for its better estimate of the elastic properties. The dramatic effect of porosities on the properties was not considered due to the uncertainties of its measurements and the low differences between the manufactured samples. The theoretical longitudinal bending modulus was computed using Eq. (4) and the theoretical transverse modulus was calculated using Eq. (5). Matrix properties were taken from the present study. Reinforcement properties are summarized in Supp.Tab.2.

$$E_{L_{th}} = V_f E_{11_f} + (1 - V_f) E_m \tag{4}$$

$$E_{T_{th}} = \frac{E_m}{1 - \sqrt{V_f}(1 - E_m / E_{22_f})} \tag{5}$$

where E_m is the matrix modulus, E_{11_f} and E_{22_f} are the fiber longitudinal and transverse modulus respectively.

2.3.2. Atomistic simulations

To estimate the complexation energies of F-PHU and F-EP assemblies and their structural characteristics, molecular mechanics and molecular dynamics simulations were first performed on isolated PHU, EP and a short fragment of cellulose (see structures in Fig. 2) with the Dreiding force field and using the Gasteiger method to assign atomic charges, as implemented in the Materials Studio package [BIOVIA, Dassault Systèmes, Materials Studio 2022, San Diego: Dassault Systèmes, 2021]. Successive quenched dynamics at different temperatures were performed until no further improvement of the total energy of the system was found. Based on the optimized structures of the isolated fragments, F-PHU and F-EP complexes were built and submitted to quenched dynamics simulations to extract their lowest energy structures. Finally, both the lowest energy structures of the isolated fragments and the complexes were re-optimized at the DFT level using the B3LYP functional, a 6-31G** basis set, and the GD3BJ Grimme's dispersion correction [29]. The reported complexation energies correspond to the energy difference between the DFT-calculated energy of the complex and the sum of the DFT-calculated energies of the isolated fragments. The reported H-bond lengths were also extracted from the DFT-optimized complexes.

3. Results and discussion

3.1. Comparison of the properties of PHU and epoxy thermosets

Before editing NFCs from PHU resins, benchmarking of the thermo-mechanical performances of neat epoxy and PHU matrices has been realized. To date, unidirectional NFCs with the highest thermo-mechanical properties are commonly achieved with epoxy-amine systems [30,31]. Switching from epoxides to cyclic carbonates implies a substantial change in terms of polymerization features, composite processing, and microstructure of the resins [32]. This questions the effect of the precursor change on the processability and final physical properties of the crosslinked polymers, especially in view of composite materials fabrication, and assesses the interest of PHU chemistry over epoxy systems.

Table 1
Comparison between epoxy and PHU neat matrices properties used for composite impregnation (mean ± standard deviation).

			Epoxy	PHU
	GC_{THF}	%	98 ± 1	99 ± 1
	ρ	g.cm^{-3}	1.19 ± 0.01	1.26 ± 0.02
Isothermal rheology 80 °C	η_{init}	Pa s	0.10	1.30
	Pot Life	min	6.5	19.0
	Gel Time	min	6.5	49.0
TGA	$T_{d_{5\%}}$	°C	315	284
	$Char_{800°C}$	%	13.3	15.2
Tensile	E	GPa	2.5 ± 0.1	2.5 ± 0.2
	σ_{yield}	MPa	55.1 ± 2.0	88.8 ± 5.1
	ε_{yield}	%	2.9 ± 0.1	4.2 ± 0.6
3Pt bending	E	GPa	2.7 ± 0.2	4.4 ± 0.1
	σ_{yield}	MPa	104.6 ± 2.7	163.5 ± 1.4
	ε_{yield}	%	5.8 ± 0.5	4.8 ± 0.3
DMA	T_α	°C	70	78
	$E'_{25°C}$	MPa	1746	3129
	$E'_{rubbery}$	MPa	23.0	6.6
	ν'_e	mol.m^{-3}	2346	657

It was previously reported that the CC conversion from epoxide led to a significant increase in the viscosity [24], likely altering its processability. To investigate this, we analyzed the curing behavior and viscosity evolution through isothermal rheology at the curing temperature of 80 °C. Figures and data related to this test can be found in the SI (Supp. Fig. 5) and Table 1. The rheological behavior of the PHU and the epoxy formulations show notable differences. The PHU displays a continuous increase in viscosity followed by a plateau with conversion progressing at a slower rate. Conversely, the low viscosity of the epoxy resin does not show any significant changes at the very beginning of the test and gelation occurs rapidly, resulting in a steady increase of the viscosity after a few minutes. It is worth noting that the initial viscosity of the PHU mixture was significantly higher than that of the epoxy formulation by a factor of 10. With a viscosity of 0.1 Pa s, the epoxy possesses a very low viscosity making it a commonly used reactive diluent and suitable for most infusion processes [31]. On the opposite, the PHU formulation presents an initial viscosity of 1.3 Pa s which rapidly increases to reach a plateau. Such particular behavior can be explained by secondary H-bonding generated during PHUs

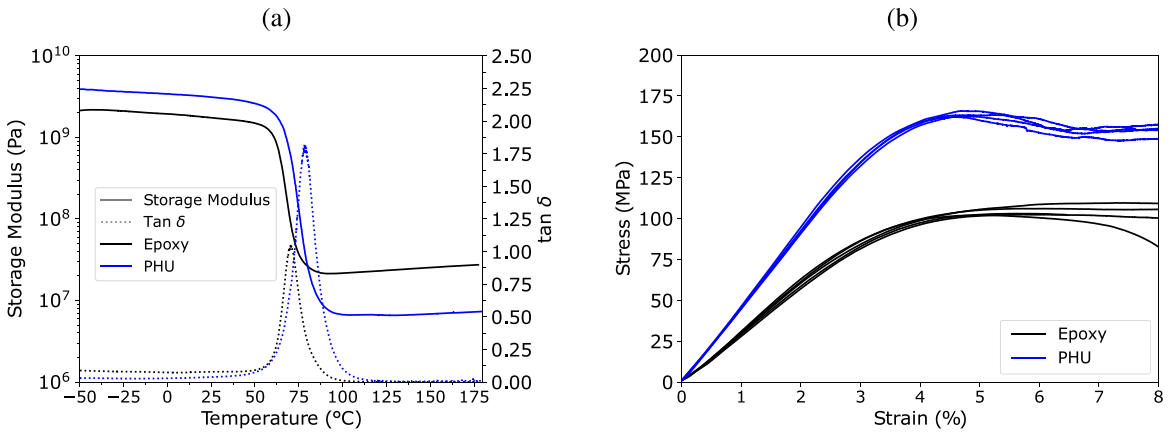

Fig. 3. (a) Thermo-mechanical behavior, and (b) three-point monotonic bending stress–strain curves of the epoxy and PHU neat matrices used for composite impregnation.

curing. These newly formed bonds result in higher viscosity, and lower reactivity due to the steric bulk hindrance effect [33]. Even though such resin can lead to elevated viscosity during curing, their curing behavior remains satisfactory for small-scale thermocompression [31,34].

Mechanical and thermo-mechanical properties of the fully cured thermosets were assessed through Dynamical Mechanical Analysis (DMA) (Fig. 3a), three-point bending (Fig. 3b), and tensile tests (Supp. Fig. 7). The thermal stability was evaluated by thermogravimetric analysis (TGA) under N_2 gas (Supp. Fig. 6). All values are reported in Table 1. Interestingly, the PHU thermoset displays a notable improvement regarding the thermo-mechanical properties. DMA highlights a superior glassy modulus at room temperature, from 1.7 GPa for the epoxy up to 3.1 GPa for the PHU. The α transition relaxation (T_α), relative to the glass transition, marks the change from the glassy domain to the rubbery domain. This transition, as determined at the maximum of the $\tan\delta$ curve, occurs at a slightly higher temperature in the case of the PHU. In particular, the PHU shows an 8 °C higher transition temperature, rising from 70 °C for the epoxy to 78 °C for the PHU. Moreover, the sharp and narrow peak in the $\tan\delta$ curve indicates a homogeneous network structure. The large intensity of the $\tan\delta$ peak of the PHU compared to the epoxy reveals drastic changes in the thermo-mechanical behavior. This heightened intensity, alongside the lower crosslinking density of PHUs, highlights the excellent damping capacities of the material [35].

This change is mainly related to the difference in the macromolecular structure of the network. Indeed, in addition to the effect of the precursor structure (aromatic, aliphatic...), it has been demonstrated that the thermo-mechanical properties of amorphous thermosets are significantly affected by the crosslinking density [36] and the hydrogen bonding [37]. Herein, the ring opening of oxirane by amines leads to secondary (primary amine reacting) and tertiary amines (secondary amines reacting) with free pendant hydroxyl groups [38]. Consequently, the resulting network is highly crosslinked with a density of 2346 $\mathrm{mol.m^{-3}}$. In contrast, for PHUs, only primary amines react with CC [12], and lead to a hydroxyurethane moiety [18]. This results in a significantly lower crosslinking density, with 657 $\mathrm{mol.m^{-3}}$. Hence, the two macromolecular structures are relatively close due to the precursor's similar structures but differ in linkage nature, crosslinking, and H-bonds density and type. These differences explain the superior thermo-mechanical properties of PHUs over epoxide counterparts at room temperature. Both H-bonds and macromolecular structure contribute to a high glassy modulus and an elevated T_α while the presence of numerous weak hydrogen bonds maintains a ductile behavior and an elevated modulus. After reaching the rubbery state, the H-bond density and strength significantly decrease and its total strength becomes insufficient, making the thermo-mechanical properties of the PHU only dictated by covalent bonding. Together with a crosslinking density of 2346 $\mathrm{mol.m^{-3}}$, the epoxy exhibits a higher rubbery storage modulus than the PHU. This behavior is also observed with both monotonic tensile and three-point bending tests. In tensile, a similar Young's modulus of 2.5 GPa is obtained for both thermosets. However, the PHU exhibits a significant increase of 61% and 47% of the stress and strain at break, respectively, over the epoxy counterpart. In three-point bending, both modulus and stress are increased in PHU by 63 and 56%, respectively, while maintaining a comparable level of ductility. It is worth noting that if the strain at yield in bending is similar, no break was reached for our PHU materials.

The different trends in tensile and bending behavior can be likely explained on the basis of other organic materials. The presence of H-bonds has been shown to increase the shearing properties of organic materials [39], explaining the higher modulus and stress during bending of the PHU compared to the epoxy counterpart. Although three-point bending tests are not supposed to exhibit shear in the Euler–Bernoulli beam theory, we cannot completely avoid it during our tests. In tensile testing, this shearing effect is not present and the lower crosslinking density of the PHU can be counterbalanced by H-bonds leading to a similar modulus. However, the macromolecular structure allows the PHU to reach higher stress and strain at break than the epoxy counterparts [37] thanks to its stronger H-bond interactions even though the crosslinking density is lower (see the modeling section below).

Regarding the thermal stability, TGA results show that the thermal degradation is almost the same with a slight increase in the char yield of the PHU over the epoxy counterpart. Overall, the study shows a significant improvement in the thermo-mechanical properties when moving from epoxy chemistry to polyhydroxyurethane chemistry. These improvements highlight the substantial advantages of utilizing carbonate derivatives as a means to readily enhance the properties of thermosets. Furthermore, the obtained thermo-mechanical properties were found to align perfectly with the requirements of NFC in the frame of high-performance matrices [31].

3.2. Evaluation of flax-PHU (F-PHU) and flax-epoxy (F-EP) structural composites

Unidirectional flax fiber laminates were then manufactured using the two studied matrices. The obtained laminates and the Scanning Electron Microscopy (SEM) images of their transversal cross-sections are depicted in Fig. 4. The density, fiber volume fraction (V_f), and void content (V_v) were calculated for each specimen and summarized in Table 2. To compare the adhesion efficiency, carbon fiber laminates were also manufactured using the epoxy and PHU matrices; their pictures and cross sections can be found in SI, and properties are summarized in Table 2.

All laminates exhibit high V_f, which are consistent with reinforcements, resulting in 50% for F-PHU, and 48% for F-EP. These values are

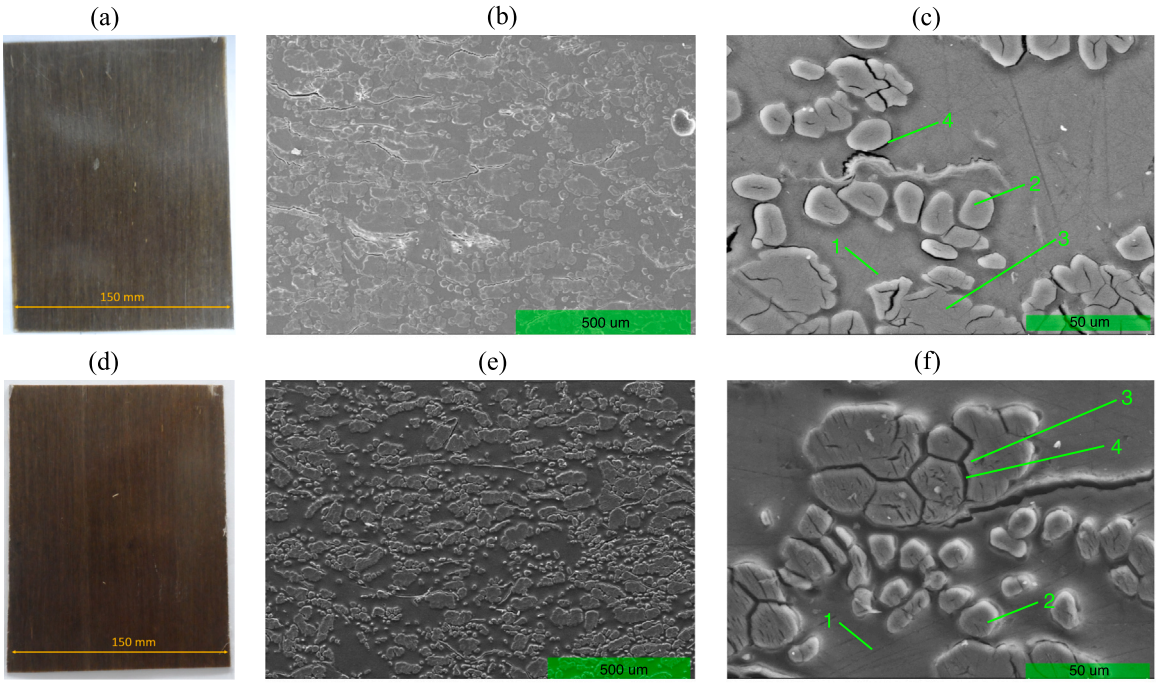

Fig. 4. Pictures of the manufactured laminates, SEM cross-section images with x80 magnifications and x700 magnifications (left to right) for (a-c) F-EP, and (d-f) F-PHU. 1: Matrix, 2: flax fiber, 3: fiber bundle, 4: adhesion discontinuity.

Table 2
Composite properties in three-point bending (mean ± standard deviation).

Load direction	Reinforcement	Matrix	ρ g.cm^{-3}	V_f %	V_v %	E GPa	σ MPa	ϵ %	E_{th} GPa	E/E_{th}
Longitudinal	Flax	EP	1.30 ± 0.01	48.4 ± 0.7	0.2 ± 0.1	27.9 ± 0.7	390.9 ± 6.9	2.39 ± 0.09	29.0	0.96
		PHU	1.31 ± 0.01	50.1 ± 3.8	1.1 ± 0.4	35.2 ± 0.6	438.2 ± 8.1	1.94 ± 0.08	30.7	1.15
	Carbon	EP	1.46 ± 0.02	52.4 ± 1.5	2.1 ± 0.2	132.4 ± 2.5	1738 ± 106	1.27 ± 0.07	127.1	1.04
		PHU	1.42 ± 0.01	46.2 ± 2.0	3.5 ± 0.2	92.6 ± 7.0	1283 ± 186	1.49 ± 0.16	113.3	0.82
Transverse	Flax	EP	1.30 ± 0.01	48.7 ± 0.4	0.2 ± 0.1	2.2 ± 0.2	25.9 ± 8	1.62 ± 0.32	5.0	0.43
		PHU	1.31 ± 0.01	51.5 ± 2.7	1.3 ± 0.3	5.4 ± 0.4	39.8 ± 4.7	0.93 ± 0.09	6.5	0.83
	Carbon	EP	1.46 ± 0.02	56.6 ± 2.2	2.6 ± 0.2	8.7 ± 0.5	83.1 ± 3.9	1.19 ± 0.09	7.4	1.18
		PHU	1.42 ± 0.01	46.3 ± 2.4	3.5 ± 0.3	7 ± 0.2	106.2 ± 7.6	1.63 ± 0.08	8.9	0.79

typical for flax composites obtained through thermocompression [27,30]. V_v range between 0.2% for F-EP to 1.1% for F-PHU, in the lower range of flax fiber composites demonstrating the high quality of the fiber impregnations [31]. The SEM images reveal well-impregnated materials with no significant differences between each other and no significant defects detected. Notably, the F-EP appears to have better-impregnated fiber bundles (Fig. 4c) due to its lower viscosity, consistent with the low porosity level. However, the SEM images reveal closer proximity at the interface in PHU-based laminates compared to epoxy-based one, suggesting a better affinity between PHUs and natural fibers [6].

To investigate the interface at the microscale, Atomic Force Microscopy (AFM) was performed, and the results are displayed in Fig. 5. Noteworthy, AFM images revealed superior wetting of the flax with the PHU matrix compared to the epoxy one. This was evident from the continuity of material observed between the flax and the PHU matrix at the interface. Despite good impregnation, the F-EP reveals discontinuity at the interface, revealing a lower affinity between the fiber and the matrix. To the author's best knowledge, it is the first time that such results have been observed in the case of NFC. Such images are consistent with the previously observed SEM images and highlight the improved affinity between PHUs and natural cellulosic fiber due to their hydrophilic character.

To gain atomistic insights into the enhanced affinity of PHUs with natural fibers compared to epoxy matrices, a modeling study combining a classical approach (molecular mechanics and molecular dynamics) and quantum calculations (Density Functional Theory, DFT) has been conducted (see Section 2.3.2). The calculations reveal higher complexation energies for PHUs with natural cellulose (−23.4 kcal/mol) in contrast to epoxy matrices (−21.2 kcal/mol). Despite the fact that both complexes feature three stabilizing hydrogen bonds, the larger complexation energy observed for PHUs with natural cellulose is attributed to the formation of these hydrogen bonds with three distinct atomic sites of cellulose, whereas in the case of epoxy matrices, the H-bonds are localized to only two atoms as shown in Fig. 6. The increase in the number of contact points on cellulose for PHU systems is a consequence of the chemical characteristics of PHU, wherein the amine and alcohol functional groups are more spatially separated compared to those in epoxy matrices. This structural difference favors increased interactions between PHUs and cellulose. Natural fibers are complex hierarchical structures composed by celluloses (crystalline and amorphous), hemicelluloses, pectins, lignin, and others [2]. Therefore for the sake of simplicity, the flax was modeled as a single repeating unit of cellulose in the atomistic simulations. As a consequence, the model should not be considered an accurate representation but an insight into the complex interactions occurring at the fiber/matrix interface. The results support the original hypothesis that implementing stronger H-bonds in the polymer backbone through this novel PHU chemistry would lead to a more intimate relationship between hydrophilic fibers and the matrix. However, a better understanding of the true interfacial interactions, chemically and physically remains required in the future of natural fiber composite to embrace their potential fully. Such work

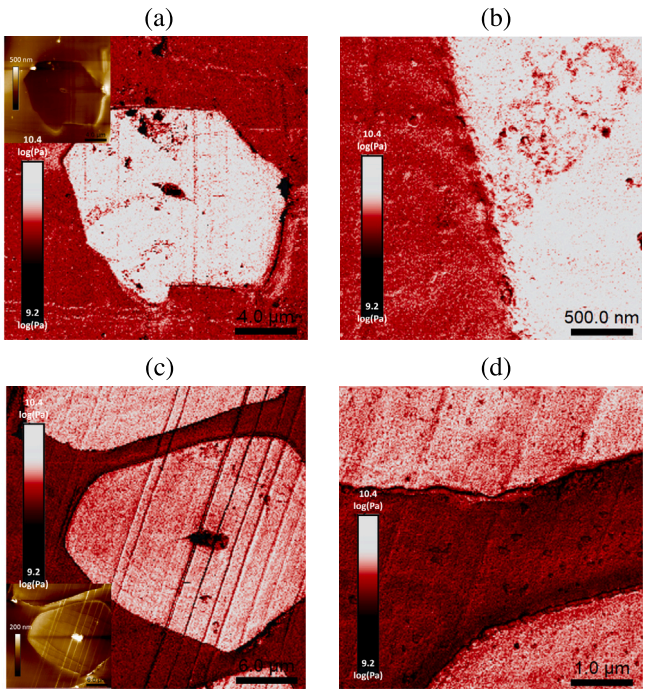

Fig. 5. (a) AFM-PFT rigidity modulus (log scale) of cryo-microtomed F-PHU sample (Inset: corresponding topographic image). (b) zoom of (a). (c) AFM-PFT rigidity modulus (log scale) of cryo-microtomed F-EP sample. (Inset: corresponding topographic image). (d) zoom of (c).

should include more detailed and representative modeling of the fiber structure.

The mechanical properties of the unidirectional laminates were assessed by three-point bending tests in the two main orthotropic directions: one with the load parallel to the fibers (referred to as F0), and one with the load perpendicular to the fibers (referred to as F90). The bending stress–strain curves of these materials are presented in Fig. 7 and a summary of their properties is shown in Table 2. It is important to note that the bending behavior is affected by the material's tensile, compressive, and shear properties. Accordingly, the failure is initiated by the weakest of these three constituents [40]. All tests consistently exhibited low dispersion and low scattering of the results, confirming the effectiveness of the processing method and the reliability of the results.

In the longitudinal direction, high bending properties were achieved for all materials, with a modulus of 28 GPa for F0-EP and an even more impressive 35 GPa for F0-PHU. Additionally, these materials displayed impressive ultimate stress values, with F0-EP reaching 391 MPa and F0-PHU achieving an even higher 438 MPa. Interestingly, the F0-PHU material exhibits remarkable modulus and admissible stress, surpassing its epoxy counterpart as well as previous studies in the literature involving similar materials [6,8,9,41,42]. In this loading direction, the matrix acts as a transferring agent of external forces to the load-bearing fibers. Therefore, it is expected that the better the interfacial adhesion, the higher the bending properties will be [6]. The strain at break of the laminates was slightly lower for PHU-based laminate (2.39% for F0-EP, 1.94% for F0-PHU). This reduction is also attributed to the improved affinity between the fibers and the matrix. In the case of lower adhesion, fiber pull-out tends to occur, resulting in a slight increase in the strain [5]. On the contrary, efficient load transfer to the fibers leads to a sharp break of both the fibers and the matrix [43]. This observation is further confirmed by the SEM images of the fractured samples, as depicted in Fig. 8 where the fibers are seen to be broken at the very failure facies for F0-PHU, while pulled-out fibers are visible on the F0-EP. Hence, these initial results provide further support for the strong affinity between PHUs and flax attributed to H-bonds, as previously stated through atomistic simulations, SEM and AFM analyses.

Despite the remarkable superiority of the F0-PHU laminate in terms of modulus and stress when compared to F0-EP, it is important to note that similar behavior and high properties were achieved for all laminates. In the longitudinal direction, the behavior is mainly governed by the reinforcement [6]. As a result, no significant differences can arise. On the opposite, in the transverse direction, the behavior is mainly brought by the matrix, and the fibers tend to act as defects [31]. Moreover, since the interfacial adhesion is directly submitted to the load in tension and compression, the transverse properties give a good insight into the interfacial strength [41]. In this transverse orientation, PHU-based laminate exhibits high-performance behavior with a bending modulus exceeding 5.0 GPa and a stress of 40 MPa. The obtained properties appear to be significantly superior to those of F90-EP, which shows a bending modulus of 2.2 GPa and a bending stress of 26 MPa. The properties obtained for F-PHU laminates are superior to equivalent materials found in literature, which exhibit properties similar to F90-EP [8,41]. This increase in performance can likely be attributed to the improved interfacial adhesion, as previously elucidated through atomistic simulations, AFM, SEM, and longitudinal bending analyses. Importantly, these observations reveal that flax-PHU composites exhibit high mechanical properties in both orthotropic directions, rendering them interesting candidates for the NFC market.

In many studies, it has been found that both V_f and porosity content significantly impact material properties [2,31]. For these reasons, Chamis' micromechanical model was applied to compare normalized moduli. The normalized value gives therefore an efficiency coefficient of adhesion [44]. Interestingly, the theoretical longitudinal modulus is comparable in all cases, with values around 30 GPa. When normalized, the ratio of the F0-EP material is 0.96. In this reference case, the ratio of moduli already highlights high compatibility and wettability between this low-viscosity amine-epoxy resin and the fiber. F-PHU laminate exhibits a ratio of 1.15, revealing important improvements in adhesion efficiency compared to the epoxy systems. These results corroborate the enhanced adhesion observed through mechanical tests and AFM analyses. For transversal properties, where the adhesion significantly affects the results, similar trends are observed. The adhesion efficiency of PHU-based materials significantly outperforms that of the epoxy-amine system. F90-EP exhibits an efficiency of 0.43, which is aligned with literature findings [31]. As observed in the longitudinal direction, the PHU matrix exhibits a significant increase in adhesion efficiency with a ratio of 0.83 for F90-PHU. These results, in addition to the first observations and mechanical results back up the original hypothesis that hydroxyurethane in the matrix would generate a stronger H-bond than epoxy amine. Such improvement leads to higher mechanical properties without requiring any fiber treatment. Therefore, the PHU matrix not only leads to an increase in both the apparent mechanical properties and calculated ones but also an increase in the adhesion strength.

Theoretically, micro-mechanical models like Chamis' assume perfect adhesion between fiber and matrix, representing an ideal material. Comparison to experimental data should lead to values lower than 1 [31]. However, the properties of natural fibers are dependent on many parameters such as the year of production, variety of flax, and fiber extraction methodology, leading to notable scattering of their properties, in particular modulus and density [2]. Therefore, the chosen values for the micromechanical model might slightly underestimate the real properties of the reinforcement. Regardless, these values still allow for meaningful comparison, especially considering that the reinforcement remains within the same range and should be taken for internal comparison within this study.

Carbon fiber composites, employing fibers specifically sized for epoxy matrices (as bought), were manufactured for comparative purposes with the NFC. Interestingly, the epoxy matrix leads to significantly better mechanical properties in both orthotropic directions when

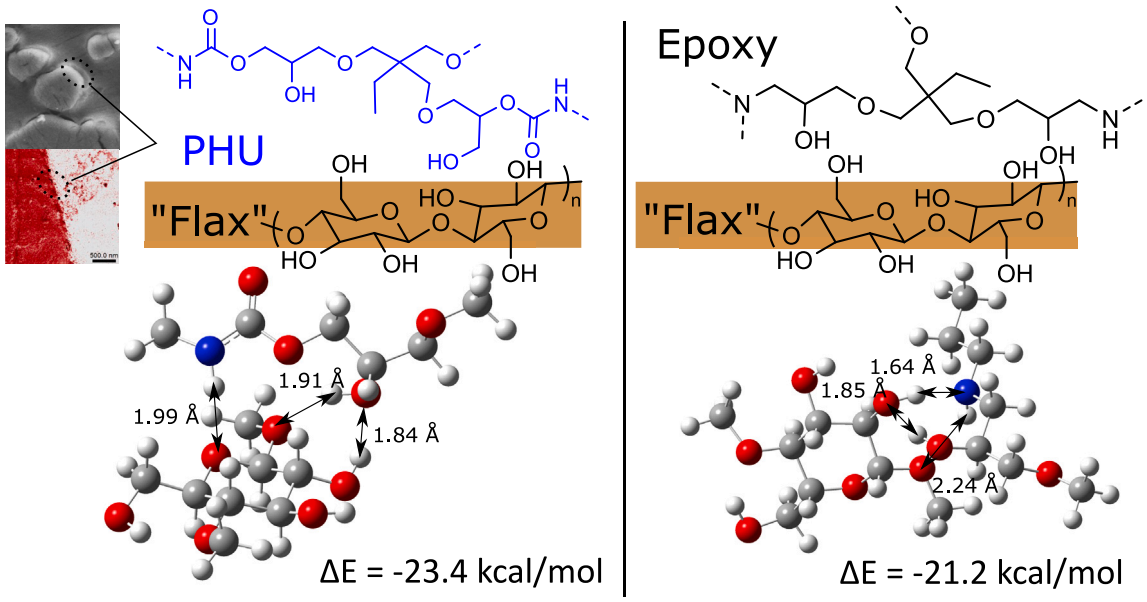

Fig. 6. Schematic representation of the interface of the composites with the DFT-optimized structure of the F-PHU (left) and F-EP(right) complexes. The numerical values correspond to the lengths of the H-Bonds between PHU or EP and the cellulose and to the DFT(B3LYP/6-31G**/GD3BJ)-calculated energies for F-PHU and F-EP.

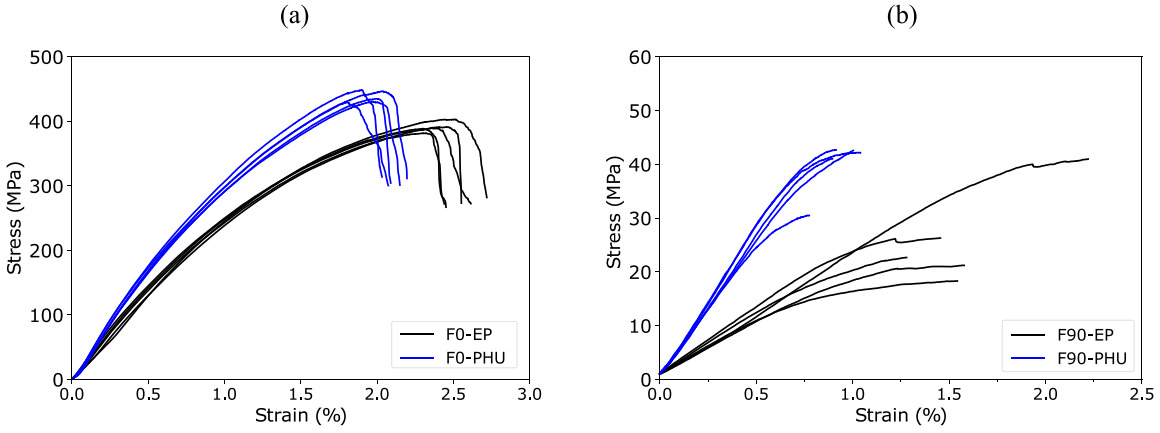

Fig. 7. Three-point bending strain–stress of F-EP and F-PHU in (a) longitudinal and (b) transverse directions.

compared with the PHU matrix, as highlighted by the stress–strain curves shown in Supp. Fig9. Moreover, in that case, the application of Chamis's model and the adhesion efficiency ratio highlights better results for epoxy-based composites. This particularly highlights the interest of PHUs to obtain high-performance NFCs without sizing agents due to the intrinsic compatibility of NF and PHUs. The theoretical model, along with monotonic bending tests, SEM images of broken samples, and AFM analyses, highlight the improved interfacial strength of PHUs with flax fibers due to better chemical and physical affinity, in addition to the good wettability.

Flax-epoxy systems are known to have poor fire resistance properties [45]. This limitation leads to several challenges when considering their use in applications such as transportation. Typically, the incorporation of halogenated or phosphorated compounds is usually required to meet fire safety standards, but this approach is questionable in terms of sustainability. Hence, we proposed here a straightforward evaluation of the flammability of flax-PHU composites following the vertical UL-94 standard. F-EP and F-PHU were tested, and the results were compared. Pictures of the tests are presented in Fig. 9. Notable differences between the two materials were observed. The F-EP materials exhibit a typical behavior of flax-epoxy material when no fire retardant is used, where large flames catch up at the ignition and propagate quickly throughout the sample, accompanied by significant smoke generation. Within less than 70 s, the material was entirely consumed by the flames, leaving behind the residual char that was too brittle to be handled, indicating the complete loss of the material's integrity during the burning test. On the opposite, Flax-PHU exhibits a smoother fire behavior. Samples required more than two minutes to get burnt, with slower flame propagation and no significant smoke generation. The residual char was stable and cohesive in a single piece, revealing the retention of some material properties and the formation of a stable protective char layer. This observation was also corroborated by TGA (Supp. Fig. 10). Although the flax-PHU material does not meet the criteria for self-extinguishing properties and is not classified as such in the test, the behavior remains enhanced compared to the epoxy counterpart. Potential dehydration and aromatization of the network could explain such behavior and should be investigated in depth to fully understand the involved mechanism.

In general, the combination of high thermo-mechanical properties, enhanced affinity between the fibers and the matrix, and the enhancement of the fire behavior through the simple addition of CO_2 in bio-epoxy opens an interesting new sustainable platform for natural fiber. These composites appear to be of high interest to the transportation industry as they offer the potential to replace petro-based polymers

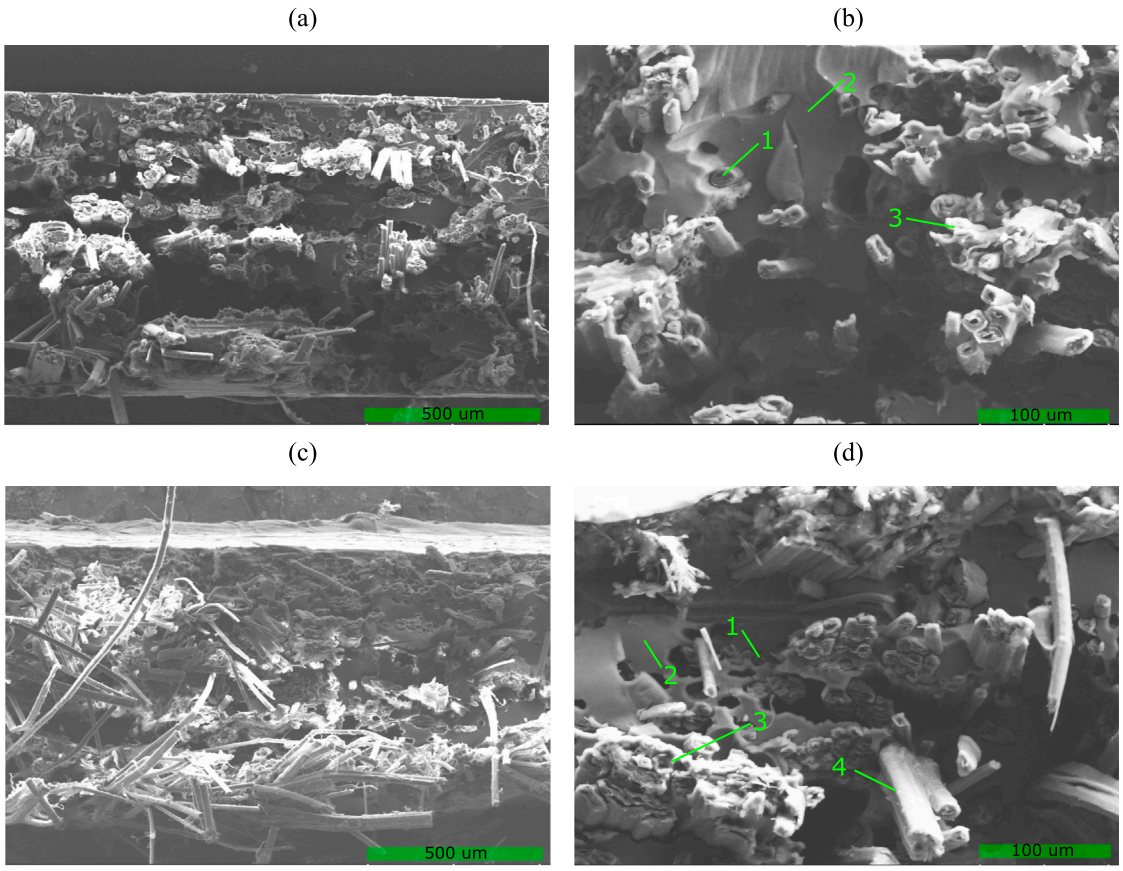

Fig. 8. Representative SEM images of the three-point bending broken samples. F0-PHU with (a) x80 and (b) x300 magnifications, and F0-EP with (c) x80 and (d) x300 magnifications. 1: Fiber break, 2: Matrix break, 3: Fiber short pull-out, 4: Fiber long pull-out.

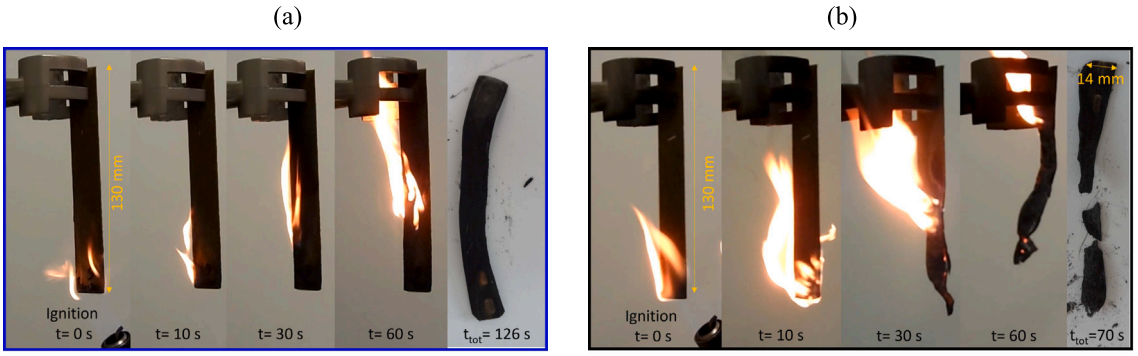

Fig. 9. Pictures of composite samples during UL94 vertical burning test. (a) F-PHU, and (b) F-EP laminates.

and improve the sustainability of composite materials with improved properties.

3.3. Welding of pre-preg PHU composites

Reprocessable thermosets constitute a significant breakthrough in the composite industry as they can provide many opportunities such as welding, reshaping, recycling of such materials, or recovery of the fibers [46]. Upon heating, hydroxyurethane functions are subjected to transcarbamoylation and dissociative reactions [15]. In transcarbamoylation, bond exchanges between hydroxyl and urethane functions allow the reprocessing of such thermosets under specific conditions without loss of crosslinking density [16]. The dissociative reaction reforms the cyclic carbonate and amine, thus leading to a decrease in the crosslink nodes [16]. These two reactions give PHU thermosets the ability to be catalyst-free reprocessed at elevated temperatures [24]. Exploiting this unique feature, single-ply F-PHU laminates were manufactured. These F-PHU sheets were then welded by thermocompression as represented in Fig. 10a.

The obtained material was smooth and homogeneous despite the harsh conditions required to weld the plies efficiently. The SEM picture presented in Fig. 10b depicts efficient welding without any observable welding line nor significative longitudinal discontinuity. When compared to the non-reprocessable epoxy material in SI (Supp. Fig. 11), which exhibits porosities, and identifiable ply lines, the SEM highlights the good welding of the plies thanks to PHU dynamic networks. Three-point bending was applied to assess the properties of the welded laminate. The curves are presented in Fig. 10c, alongside the F0-PHU manufactured in the previous section as a reference. The welded composite exhibits a modulus of 30 GPa, a stress of 213 MPa, and

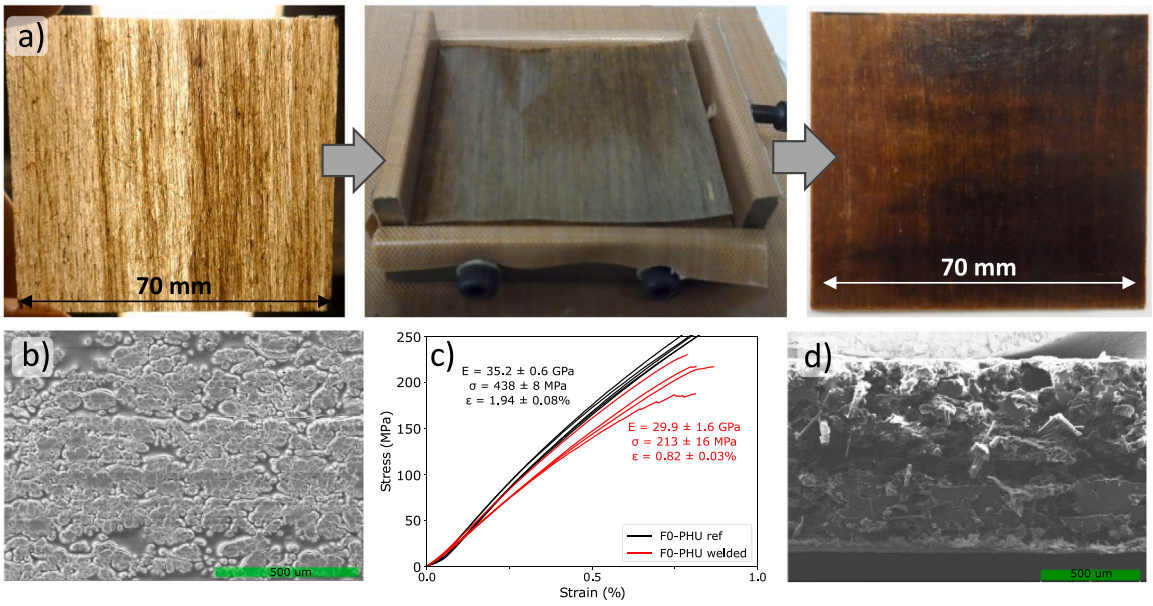

Fig. 10. (a) Welding process of flax-PHU laminate. From left to right, single-ply cured sheet, stacking in the mold and cured plate. (b) SEM of the welded composite cross-section, (c)Three-point bending strain–stress curves of the welded F-PHU composite in the longitudinal direction, (c) failure facies of the three-point bending specimen with x70 magnification.

a strain at break of 0.82%. The results are only slightly scattered, revealing the overall material homogeneity and the reliability of the process. The high modulus emphasizes the effectiveness of the welding process [47]. Moreover, the failure facies presented in Fig. 10d disclose neat and brittle failure of the fibers, leading to the catastrophic failure of the entire material with no delamination observed. This further highlights the efficacy of the welding process [47].

It is important to note that despite the rather good ultimate properties obtained compared to other works in the literature [30] and the effectiveness of the welding, the laminate experienced a significant drop in the ultimate properties, approximately 50%, compared to the original material. This decrease can be attributed to the thermal degradation of the fibers as stated in literature [2]. Prolonged exposure to elevated temperature leads to a drastic change in the microstructure of the fibers and their chemical composition, and thus embrittlement.

However, the welding of the flax-PHU composite must be seen as a proof-of-concept, showcasing a specific added feature derived from the shift of chemistry from epoxides to polyhydroxyurethanes. Here, the materials were processed under catalyst-free conditions. Further exploration of optimized reprocessing conditions, catalysts, formulations, and recycling methods [17] are expected to yield even more promising outcomes. Such features open doors to the implementation of bio-based recyclable structural composite with improved properties.

4. Conclusions

Despite the growing interest in natural fibers as reinforcement of polymer matrix composites, the sustainability and compatibility of the matrix used remain an issue. This work addresses such issues through the development of sustainable matrices with enhanced properties using non-isocyanate polyurethane chemistry. In particular, polyhydroxyurethanes (PHU) were synthesized from bio- and CO_2- derived cyclic carbonates and diamine. The physical properties of the neat PHU were measured and compared to a similar epoxy network. PHUs exhibit superior thermo-mechanical properties with a glass transition temperature above 78 °C and a bending modulus exceeding 4 GPa. The obtained properties were found to align with the requirements for structural natural fiber composites.

For the first time, PHU was used to manufacture flax fibers' unidirectional laminates. The results indicated homogeneous impregnation and enhanced wetting of the fiber with PHU compared to epoxy, as confirmed by AFM measurements and rationalized via atomistic simulations. The bending properties were among the highest reported in the literature, with a modulus of 35 GPa, and ultimate stress and strain of 440 MPa and 1.94% respectively. Interestingly, when normalizing results through Chami's micromechanical model, PHU-based composites outperform epoxy ones by nearly 30%. Such an increase was found to be specific to the natural fiber-PHU material as carbon fiber composites were superior using epoxy resins. Taking advantage of the inherent dynamic urethane linkages, we successfully manufactured cured pre-impregnated laminates that were further welded to create the final material. While this welding process has potential, further optimization is required.

Polyhydroxyurethanes appear as a new sustainable platform suitable for the composite industry, particularly for applications in the transportation market. PHUs however remain an emerging polymer and comprehensive studies regarding the durability, aging, and environmental conditions should be performed to facilitate the widespread adoption of PHU-Natural fiber composites. The reprocessing and recycling of the final material should be also investigated in depth. The observed viscosity may pose a potential limitation for scaling up the manufacturing of such sustainable materials, a challenge that we plan to investigate in future research work.

CRediT authorship contribution statement

Guillem Seychal: Writing – original draft, Visualization, Investigation, Formal analysis, Data curation, Conceptualization. **Pierre Nickmilder:** Investigation. **Vincent Lemaur:** Writing – review & editing, Software, Investigation. **Connie Ocando:** Writing – review & editing, Supervision, Project administration, Funding acquisition. **Bruno Grignard:** Writing – review & editing, Resources, Methodology. **Philippe Leclère:** Writing – review & editing, Resources, Methodology. **Christophe Detrembleur:** Writing – review & editing, Supervision, Resources. **Roberto Lazzaroni:** Writing – review & editing, Software, Resources. **Haritz Sardon:** Writing – review & editing, Supervision. **Nora Aranburu:** Writing – review & editing, Supervision, Resources, Conceptualization. **Jean-Marie Raquez:** Writing – review & editing, Supervision, Project administration, Funding acquisition, Conceptualization.

Declaration of competing interest

The authors declare that they have no known competing financial interests or personal relationships that could have appeared to influence the work reported in this paper.

Data availability

Data will be made available on request.

Acknowledgments

The authors would like to thank the financial support provided by the NIPU-EJD project; this project has received funding from the European Union's Horizon 2020 research and innovation program under the Marie Skłodowska-Curie grant agreement No 955700. JM.R. and C.D. thank F.R.S.-FNRS, Belgium for funding. The research at LPNE is partly supported by F.R.S. – FNRS PDR Project, Belgium (40007942) and F.R.S. – FNRS Grands Equipements Project (40007941) (Belgium). The modeling activities in Mons are supported by FNRS, Belgium (Consortium des Equipements de Calcul Intensif – CECI, under Grant 2.5020.11) and by the Walloon Region, Belgium (ZENOBE and LUCIA Tier-1 supercomputers, under grant 1117545).

Appendix A. Supplementary data

Supplementary material related to this article can be found online at https://doi.org/10.1016/j.compositesa.2024.108311.

References

[1] Mutel F. Flax and hemp fiber composites, a market reality: The biobased solutions for the industry. JEC Group; 2018.
[2] Bourmaud A, Beaugrand J, Shah DU, Placet V, Baley C. Towards the design of high-performance plant fibre composites. Prog Mater Sci 2018;97:347–408.
[3] Le Duigou A, Davies P, Baley C. Environmental impact analysis of the production of flax fibres to be used as composite material reinforcement. J Biobased Mater Bioenergy 2011;5(1):153–65
[4] Le Moigne N, Otazaghine B, Corn S, Angellier-Coussy H, Bergeret A. Modification of the interface/interphase in natural fibre reinforced composites: Treatments and processes. In: Surfaces and interfaces in natural fibre reinforced composites. Cham: Springer International Publishing; 2018, p. 35–70.
[5] Le Duigou A, Kervoelen A, Le Grand Ad, Nardin M, Baley C. Interfacial properties of flax fibre–epoxy resin systems: Existence of a complex interphase. Compos Sci Technol 2014;100:152–7.
[6] Sarkar F, Akonda M, Shah DU. Mechanical properties of flax tape-reinforced thermoset composites. Materials 2020;13(23):5485.
[7] Andrew JJ, Dhakal H. Sustainable biobased composites for advanced applications: recent trends and future opportunities – A critical review. Composites C: Open Access 2022;7:100220.
[8] Jeannin T, Gabrion X, Ramasso E, Placet V. About the fatigue endurance of unidirectional flax-epoxy composite laminates. Composites B 2019;165:690–701.
[9] Seychal G, Ramasso E, Le Moal P, Bourbon G, Gabrion X, Placet V. Towards in-situ acoustic emission-based health monitoring in bio-based composites structures: Does embedment of sensors affect the mechanical behaviour of flax/epoxy laminates? Composites B 2022;236(3):109787.
[10] Bobade SK, Paluvai NR, Mohanty S, Nayak SK. Bio-based thermosetting resins for future generation: A review. Polym-Plast Technol Eng 2016;55(17):1863–96
[11] Zhang J, Chevali VS, Wang H, Wang CH. Current status of carbon fibre and carbon fibre composites recycling. Composites B 2020;193:108053.
[12] Carré C, Ecochard Y, Caillol S, Averous L. From the synthesis of biobased cyclic carbonate to polyhydroxyurethanes: a promising route towards renewable NonIsocyanate Polyurethanes. ChemSusChem 2019;12(15):3410–30.
[13] Maisonneuve L, Lamarzelle O, Rix E, Grau E, Cramail H. Isocyanate-free routes to polyurethanes and poly(hydroxy urethane)s. Chem Rev 2015;115(22):12407–39
[14] Aomchad V, Cristofol A, Monica FD, Limburg B, D'Elia V, W. Kleij A. Recent progress in the catalytic transformation of carbon dioxide into biosourced organic carbonates. Green Chem 2021;23(3):1077–113.
[15] Bakkali-Hassani C, Berne D, Ladmiral V, Caillol S. Transcarbamoylation in polyurethanes: Underestimated exchange reactions? Macromolecules 2022;55(18):7974–91.
[16] Chen X, Li L, Jin K, Torkelson JM. Reprocessable polyhydroxyurethane network exhibiting full property recovery and concurrent associative and dissociative dynamic chemistry via transcarbamoylation and reversible cyclic carbonate aminolysis. Polymer Chem 2017;8(6349):6349–55.
[17] Bakkali-Hassani C, Berne D, Bron P, Irusta L, Sardon H, Ladmiral V, et al. Polyhydroxyurethane covalent adaptable networks: looking for suitable catalysts. Polymer Chem 2023;14(31):3610–20
[18] Khatoon H, Iqbal S, Irfan M, Darda A, Rawat NK. A review on the production, properties and applications of non-isocyanate polyurethane: A greener perspective. Prog Org Coat 2021;154:106124.
[19] Helbling P, Hermant F, Petit M, Vidil T, Cramail H. Design of plurifunctional cyclocarbonates and their use as precursors of poly(hydroxyurethane) thermosets: A review. Macromol Chem Phys 2023;224(23):2300300.
[20] Fleischer M, Blattmann H, Mülhaupt R. Glycerol-, pentaerythritol- and trimethylolpropane-based polyurethanes and their cellulose carbonate composites prepared via the non-isocyanate route with catalytic carbon dioxide fixation. Green Chem 2013;15(4):934
[21] Panchireddy S, Grignard B, Thomassin J-M, Jerome C, Detrembleur C. Bio-based poly(hydroxyurethane) glues for metal substrates. Polymer Chem 2018;9(19):2650–9
[22] Gomez-Lopez A, Panchireddy S, Grignard B, Calvo I, Jerome C, Detrembleur C, et al. Poly(hydroxyurethane) adhesives and coatings: State-of-the-art and future directions. ACS Sustain Chem Eng 2021;9(29):9541–62.
[23] Bourguignon M, Grignard B, Detrembleur C. Water-induced self-blown non-isocyanate polyurethane foams. Angew Chem, Int Ed 2022;61(51):1–10
[24] Seychal G, Ocando C, Bonnaud L, De Winter J, Grignard B, Detrembleur C, et al. Emerging polyhydroxyurethanes as sustainable thermosets: A structure–property relationship. ACS Appl Polymer Mater 2023;5(7):5567–81
[25] Baroncini EA, Kumar Yadav S, Palmese GR, Stanzione JF. Recent advances in bio-based epoxy resins and bio-based epoxy curing agents. J Appl Polym Sci 2016;133(45):app.44103
[26] Scodeller I, Mansouri S, Morvan D, Muller E, De Oliveira Vigier K, Wischert R, et al. Synthesis of renewable m-Xylylenediamine from biomass-derived furfural. Angew Chem 2018;130(33):10670–4
[27] Cadu T, Berges M, Sicot O, Person V, Piezel B, Van Schoors L, et al. What are the key parameters to produce a high-grade bio-based composite? Application to flax/epoxy UD laminates produced by thermocompression. Composites B 2018;150:36–46.
[28] Sendeckyj G, Wang S, Steven Johnson W, Stinchcomb W, Chamis C. Mechanics of composite materials: Past, present, and future. J Compos Technol Res 1989;11(1):3.
[29] Grimme S, Ehrlich S, Goerigk L. Effect of the damping function in dispersion corrected density functional theory. J Comput Chem 2011;32(7):1456–65
[30] Pickering K, Efendy MA, Le T. A review of recent developments in natural fibre composites and their mechanical performance. Composites A 2016;83:98–112.
[31] Shah DU. Developing plant fibre composites for structural applications by optimising composite parameters: a critical review. J Mater Sci 2013;48(18):6083–107
[32] Panchireddy S. Transformation of CO2 into high performance polyhydroxyurethane adhesives and coatings [Ph.D. thesis], ULiège - Université de Liège; 2018.
[33] Blain M, Cornille A, Boutevin B, Auvergne R, Benazet D, Andrioletti B, et al. Hydrogen bonds prevent obtaining high molar mass PHUs. J Appl Polym Sci 2017;134(45):44958.
[34] Advani SG, Hsiao KT. 1 - Introduction to composites and manufacturing processes. In: Advani SG, Hsiao K-T, editors. Manufacturing techniques for polymer matrix composites. Woodhead publishing series in composites science and engineering, Elsevier. Woodhead Publishing; 2012, p. 1–12.
[35] Duc F, Bourban P, Plummer C, Månson J-A. Damping of thermoset and thermoplastic flax fibre composites. Composites A 2014;64:115–23.
[36] Shokuhfar A, Arab B. The effect of cross linking density on the mechanical properties and structure of the epoxy polymers: molecular dynamics simulation. J Mol Model 2013;19(9):3719–31
[37] Li W, Ma J, Wu S, Zhang J, Cheng J. The effect of hydrogen bond on the thermal and mechanical properties of furan epoxy resins: Molecular dynamics simulation study. Polym Test 2021;101:107275.
[38] Wang X, Gillham JK. Competitive primary amine/epoxy and secondary amine/epoxy reactions: Effect on the isothermal time-to-vitrify. J Appl Polym Sci 1991;43(12):2267–77
[39] Saha S, Mishra MK, Reddy CM, Desiraju GR. From molecules to interactions to crystal engineering: Mechanical properties of organic solids. Acc Chem Res 2018;51(11):2957–67
[40] Meng M, Le HR, Rizvi MJ, Grove SM. 3D FEA modelling of laminated composites in bending and their failure mechanisms. Compos Struct 2015;119:693–708.
[41] Hallak Panzera T, Jeannin T, Gabrion X, Placet V, Remillat C, Farrow I, et al. Static, fatigue and impact behaviour of an autoclaved flax fibre reinforced composite for aerospace engineering. Composites B 2020;197:108049.

[42] Seychal G, Van Renterghem L, Ocando C, Bonnaud L, Raquez JM. Towards sustainable reprocessable structural composites: Benzoxazines as biobased matrices for natural fibers. Composites B 2024;272:111201.
[43] Monti A, El Mahi A, Jendli Z, Guillaumat L. Mechanical behaviour and damage mechanisms analysis of a flax-fibre reinforced composite by acoustic emission. Composites A 2016;90:100–10.
[44] Madsen B, Thygesen A, Lilholt H. Plant fibre composites – porosity and stiffness. Compos Sci Technol 2009;69(7–8):1057–69.
[45] Saba N, Jawaid M, Paridah MT, Al-othman OY. A review on flammability of epoxy polymer, cellulosic and non-cellulosic fiber reinforced epoxy composites: Flammability of epoxy polymer and its composites. Polym Adv Technol 2015;27(5):577–90.
[46] Schenk V, Labastie K, Destarac M, Olivier P, Guerre M. Vitrimer composites: current status and future challenges. Mater Adv 2022;3(22):8012–29.
[47] An L, Li X, Jin C, Zhao W, Shi Q. An extrinsic welding method for thermosetting composites: Strong and repeatable. Composites B 2022;245:110224.